Bortezomib Inhibits Nuclear Factor-κB–Dependent Survival and Has Potent *In vivo* Activity in Mesothelioma

Andrea Sartore-Bianchi,[1] Fabio Gasparri,[2] Arturo Galvani,[2] Linda Nici,[3] James W. Darnowski,[3] Dario Barbone,[4] Dean A. Fennell,[5] Giovanni Gaudino,[4] Camillo Porta,[1] and Luciano Mutti[6]

Abstract

Purpose: Purpose of this study has been the assessment of nuclear factor-κB (NF-κB) as a survival factor in human mesothelial cells (HMC), transformed HMC and malignant mesothelioma (MMe) cells. We aimed at verifying whether the proteasome inhibitor Bortezomib could abrogate NF-κB activity in MMe cells, leading to tumor cell death and may be established as a novel treatment for this aggressive neoplasm.

Experimental Design: In HMC and MMe cells, NF-κB nuclear translocation and DNA binding were studied by electrophoretic mobility shift assay, following treatment with tumor necrosis factor-α (TNF-α). The IKK inhibitor Bay11-7082 was also tested to evaluate its effects on HMC, transformed HMC, and MMe cell viability upon exposure to asbestos fibers. Following Bortezomib treatment, cytotoxicity of MMe cells was evaluated by 3-(4,5-dimethylthiazol-2-yl)-2,5-diphenyltetrazolium bromide, whereas apoptosis and cell-cycle blockade were investigated by high-content analysis. Bortezomib was also given to mice bearing i.p. xenografts of MMe cells, and its effects on tumor growth were evaluated.

Results: Here, we show that NF-κB activity is a constitutive survival factor in transformed HMC, MMe cells, and acts as a survival factor in HMC exposed to asbestos fibers. Bortezomib inhibits NF-κB activity in MMe cells and induces cell cycle blockade and apoptosis *in vitro* as well as tumor growth inhibition *in vivo*.

Conclusions: Inhibition of NF-κB constitutive activation in MMe cells by Bortezomib resulted in *in vitro* cytotoxicity along with apoptosis and *in vivo* tumor regression. Our results support the use of Bortezomib in the treatment of MMe and has led to a phase II clinical trial currently enrolling in Europe.

Malignant Mesothelioma (MMe) is a primary pleural and peritoneal cancer related to asbestos exposure. Epidemiologic data show that in the next 30 years, this disease will cause a quarter of a million of deaths in Europe in men who have been occupationally exposed to asbestos fibers (1). In the United States, MMe has already increased in frequency by 90% during the last two decades, and currently, ~4,000 deaths per year are attributed to this disease (2). Rarely suitable for radical surgical resection and usually resistant to both radiotherapy and chemotherapy, MMe is denoted by a very poor prognosis, with a median survival of 12 to 18 months from diagnosis (3). Clearly, effective systemic treatment options are needed for this disease.

Among the numerous factors involved in the resistance of cancer cells to death, the transcriptional factor NF-κB seems to play a relevant role. NF-κB promotes cell survival by activating transcription of target genes normally repressed by binding of the specific inhibitor IκB, which sequesters the NF-κB p50/p65 heterodimer in the cytoplasm (4). Inhibition is reversed in response to several intracellular stimuli, resulting in targeted, ubiquitin/proteasome-mediated degradation of IκB (5, 6). Free NF-κB then translocates to the nucleus to activate genes protecting the cell from apoptosis, promoting cell growth and differentiation, and inducing synthesis of angiogenic factors (4). Deregulation of NF-κB signaling control is an important feature of a number of human hematological malignancies and solid tumors, including head and neck, pancreatic, colon, breast, and non–small cell lung carcinomas (7–12). Moreover, activation of the NF-κB pathway can stimulate proliferation and reduce the effectiveness of chemotherapy and ionizing radiation (13, 14).

Bortezomib (already known as PS-341, Velcade™) is a potent and selective inhibitor of the 20S proteasome (15). The actions of Bortezomib are pleiotropic and include inhibition of NF-κB activation by preventing IκB degradation. *In vitro* and mouse

Authors' Affiliations: [1]Falck Division of Medical Oncology, Niguarda, Ca' Granda Hospital, Milan, Italy; [2]Oncology, Biology Department, Nerviano Medical Sciences, 20014 Nerviano, Italy; [3]Division of Hematology/Oncology, Department of Medicine, Rhode Island Hospital and Brown University, Providence, Rhode Island; [4]Dipartimento di Scienze Chimiche, Alimentari, Farmaceutiche e Farmacologiche and Drug and Food Biology Center, University of Piemonte Orientale "A. Avogadro", 28100 Novara, Italy; [5]Center for Cancer Research and Cell Biology, Queen's University, Belfast, N. Ireland, United Kingdom; and [6]Local Health Unit 11, Vercelli, Italy

Received 3/3/07; revised 6/15/07; accepted 7/10/07.

Grant support: The Buzzi Foundation for the Study of Malignant Mesothelioma (Casale Monferrato, Italy) and Associazone Italiana per la Ricerca sul Cancro.

The costs of publication of this article were defrayed in part by the payment of page charges. This article must therefore be hereby marked *advertisement* in accordance with 18 U.S.C. Section 1734 solely to indicate this fact.

Requests for reprints: Luciano Mutti, Lab of Clinical Oncology, Department of Medicine, Local Health Unit 11 Vercelli P. le Lora 1 13011 Borgosesia (VC), Italy. Phone: 39-0163-203-7240; E-mail: luciano.mutti@hotmail.it.

doi:10.1158/1078-0432.CCR-07-0536

xenograft studies have clearly shown that this molecule possesses antitumor activity in a variety of human cancers (16), and Bortezomib received approval from the U.S. Food and Drug Administration (FDA), for second-line therapy of patients with progressive multiple myeloma. The importance of the ubiquitin proteasome system has been identified in peritoneal mesothelioma cells where Bortezomib, in combination with oxaliplatin, has shown preclinical activity (17); similarly, another proteasome inhibitor (PSI) has demonstrated *in vitro* efficacy on MMe cells (18).

Here, we report that NF-κB acts as a survival factor in human mesothelial cells (HMC) exposed to asbestos fibers, and that Bortezomib antagonizes constitutive NF-κB activity in MMe cells, exerting *in vitro* cytotoxicity. Evidence is provided for the first time *in vivo*, demonstrating potent activity of Bortezomib against MMe xenografts. These results have provided a rationale for using Bortezomib as a novel treatment for MMe therapy, which is currently being evaluated in European multicenter phase II clinical trials.

Materials and Methods

Cell lines and culture conditions. The malignant mesothelioma cell line REN was generously provided from Dr. Steven Albelda (University of Pennsylvania, Philadelphia, PA; ref. 19). The MMB and MMP cell lines have been derived from pleural effusions of patients with MMe and stabilized in culture. Normal HMCs are an early-passage primary cell line derived from transudative pleural fluid of a patient with heart failure. Mesothelial origin of all the lines was confirmed by immunocytochemistry using antibodies against cytokeratin, vimentin, calretinin, and carcinoembryonic antigen (CEA). A profile of cytokeratin, vimentin, calretinin positivity, and CEA negativity was established as criteria of mesothelial origin, as previously described (20). MMe cells were maintained in RPMI 1640 containing 10% fetal bovine serum (FBS), whereas HMC cells were cultured using OptiMEM containing 20% FBS. All cell lines were cultured at 37° in a humidified incubator in an atmosphere of 5% CO_2. Under these growth conditions, the doubling time was ~24 h for the REN, MMB, and MMP cell lines and ~36 h for HMC.

Asbestos fibers. Amosite fibers from the Unio Internationale Contra Cancrum were suspended in PBS at 2.0 mg/mL and then triturated eight times through a 22-gauge needle and autoclaved. Cells were cultured for 24 h in medium containing 2% FBS, supplemented with 10 μg/cm^2 amosite fibers. Also, a long-term exposure was done by culturing cells for 60 days, after two cycles of treatment, 72 h each, with low concentrations (2 or 5 μg/cm^2) of amosite fibers, as previously described (20).

Drug and reagents. For *in vitro* studies, Bortezomib (Millennium Pharmaceutical Inc.) was reconstituted in DMSO at a concentration of 1 mmol/L and serially diluted in normal saline to achieve a concentration of 1 μmol/L. For *in vivo* evaluation of antitumor activity, injectable Bortezomib (3.5 mg per 10-mL vial) was diluted in normal saline to achieve a solution of 25 μg/mL. Mice received i.p. injections of 100 μL per 2.5 g of mouse body weight or 50 μL per 2.5 g of body weight of this solution to achieve doses of 1.0 or 0.5 mg/kg, respectively. *In vitro* studies of the signaling pathway leading to NF-κB binding activity were done using inhibitors of phosphoinositide-3-kinase (PI3K; wortmannin), Erk2 (PD98059), p38 (PD169316), c-Src (PP2), and IKK (Bay 11-7082), all from Sigma. Serum-starved cells were treated with purified recombinant human HGF (50 ng/mL; R&D Systems Inc.) for 15 min in serum-free medium. For the NF-κB nuclear translocation assay, the exportin inhibitor leptomycin B (LMB; from Sigma) was used as a control.

RPMI 1640 cell culture growth medium, trypsin, and FBS were purchased from Life Technologies. Electrophoretic mobility shift assay (EMSA) reagents and the probe set for NF-κB were purchased from Panomics. Monoclonal antibodies to phospho–NF-κB antibodies were purchased from Cell Signaling Technology, whereas human poly(ADP-ribose)-polymerase (PARP) was purchased from Zymed Laboratories. Reagents for SDS-PAGE were purchased from Bio-Rad Laboratories. For immunocytochemistry, anti-active caspase-3 antibody was purchased from Promega; anti-cyclin B1 antibody and monoclonal anti–NF-κB p65^{RelA} antibody were purchased from Santa Cruz Biotechnology; anti-rabbit Cy™2- and anti-mouse Cy™5-conjugated secondary antibodies were obtained from Amersham Biosciences; anti-bromodeoxyuridine (BrdUrd) antibody and nuclease reagent were obtained within the Cell Proliferation Fluorescence Kit (Amersham Biosciences); recombinant tumor necrosis factor-α (TNF-α), BrdUrd, and 4′,6-diamidino-2-phenylindole (DAPI) were obtained from Sigma-Aldrich. All other chemicals were purchased from Sigma.

Cytotoxicity assay. Evaluation of the cytotoxic effect of Bortezomib was done using the 3-(4,5-dimethylthiazol-2-yl)-2,5-diphenyltetrazolium bromide (MTT)–based semiautomated colorimetric assay that assessed mitochondrial activity. Briefly, 3×10^3 cells were plated into each well of a 96-well flat-bottom plate (Costar, Corning Incorporated) in 100 μL of RPMI 1640 containing 10% FBS. After 24 h, Bortezomib was added to each well to achieve a final concentration of 0 to 100 nmol/L. After an additional 72 h, 100 μL of a 5-mg/mL MTT solution diluted in PBS was added to each well, and the plate was incubated for 2 h at 37°C. Plates were centrifuged at 200 × *g* for 10 min, and the resulting supernatant in each well was aspirated and replaced with 100 μL of DMSO. After gentle shaking for 5 min, the absorbance of each well at 550 nm was determined using a Dynatech MR-500 plate reader. Cells not exposed to the drug or medium containing no cells were used as positive or negative controls, respectively. An absorbance twice that of the negative control was considered positive for the presence of viable cells.

Fluorescence immunocytochemistry and high-content analysis. Cells were seeded at a density of 8×10^3 cells per well in 96-well poly-L-lysine–coated clear-bottomed plates (Matrix Technologies) and cultured overnight. After treatment with compounds for the indicated time points, 50 μmol/L BrdUrd was added to the medium for 15 to 20 min, and then cells were fixed with 3.7% (v/v) formaldehyde for 20 min and permeabilized with 0.3% (v/v) Triton X-100 (Sigma-Aldrich) in PBS for 15 min. Cells were alternatively immunostained with anti-BrdUrd, anti–cyclin B1, and anti-active caspase-3 antibodies and counterstained with DAPI. BrdUrd incorporation and cyclin B1 represent well-characterized markers of active S-phase and G_2-M phase, respectively (21), whereas active caspase-3 is a specific apoptotic marker (22). For immunostaining procedure, cells were saturated with 1% (w/v) bovine serum albumin (BSA) for 1 h, and then primary antibody was added at the manufacturer's recommended dilution in PBS containing 1% (w/v) BSA and 0.3% (v/v) Tween-20 (Sigma-Aldrich) for 1 h at 37°C. The antibody solution was removed, and cells were washed twice with PBS. For BrdUrd incorporation analysis, anti-BrdUrd primary antibody was added diluted 1:100 in nuclease solution. Cells were then washed twice with PBS, and secondary antibody was added diluted 1:500 in PBS containing 1% (w/v) BSA, 0.3% (v/v) Tween-20, and 1 μg/mL DAPI for 1 h at 37°C. After incubation, cells were washed twice with PBS, and 200 μL PBS were left in each well. The ArrayScan HCA reader (Thermo Fisher Scientific Inc.), used to quantify cellular parameters by fluorescence staining, has been previously described (21). A quadruple band fluorescence XF93 excitation filter (Omega Optical) was used to acquire images in the DAPI, green or far-red channels with a 10× objective by exposing fields for fixed times. For each sample, at least 10 fields were automatically acquired and analyzed by the ArrayScan software, corresponding to at least 500 cells. Each single cell was recognized, counted, and accepted for subsequent analysis on the basis of its nuclear DAPI fluorescence. The Cytotoxicity I and Nuclear Translocation bioapplications (Thermo Fisher Scientific Inc.) were used to quantify the intensity of nuclear and cytoplasmic fluorescence in each single cell. Cell number was also

quantified for each dose of compound on the basis of their nuclear DAPI staining and reported as percentage of cells scored in 10 fields with respect to untreated controls (normalized at 100%). EC_{50} values were estimated from dose-response curves by nonlinear regression analysis.

EMSA. DNA binding of NF-κB in HMC and MMe cells (3 to 5 × 10^6) was evaluated at basal conditions (MMP, MMB, and REN versus MLP29) following exposure either to asbestos fibers in medium (MMB and REN), in the presence or absence of Bay 11-7082 or in medium containing 25 and 100 nmol/L Bortezomib up to 48 in comparison with Bay 11-7082 (MMB and REN). Nuclear extracts were prepared as previously described (23). About 5 μg of the nuclear extract were preincubated for 10 min at room temperature in binding buffer [50 mmol/L Tris-HCl (pH 7.4), 250 mmol/L NaCl, 2.5 mmol/L EDTA, 2.5 mmol/L DTT, 20% glycerol, 5 mmol/L $MgCl_2$] supplemented with 2 μg of poly(dI-dC)•poly(dI-dC); Amersham. This mixture was subsequently incubated in a total volume of 20 μL at room temperature with γ-^{32}P-ATP–labeled oligonucleotide probe (Promega Corporation), corresponding to the human consensus NF-κB site. DNA-protein complexes were resolved on a 6% nondenaturing polyacrylamide gel in 0.5% Tris-borate-EDTA, and the labeled complexes were visualized by autoradiography.

NF-κB nuclear translocation analysis. NF-κB $p65^{RelA}$ translocation across the nuclear envelope was analyzed in MMP and REN cells by high-content analysis (HCA). Pretreatment with inhibitors was done for 4, 8, or 24 h, then 4 ng/mL TNF-α was added, and cells were incubated with inhibitors for an additional 1 h.

After treatments for the indicated times, cells were immunostained with an anti–NF-κB antibody and counterstained with DAPI. The ArrayScan reader was used to acquire images of at least 200 cells in each sample and to quantify the difference between the intensity of nuclear and cytoplasmic NF-κB–associated fluorescence (Nuc-Cyto Diff), reported as translocation parameter as previously described (24).

Immunoblotting. About 1 × 10^6 cells were seeded into separate 75-cm^2 tissue culture flasks containing 20 mL of medium plus serum. Twenty-four hours later, Bortezomib was added at concentrations of 0 to 100 nmol/L. Cells were harvested by trypsinization 24 and 48 h after the addition of the drug, and cell extracts were prepared in a cell lysis buffer containing 50 mmol/L Tris (pH, 7.4), 150 mmol/L NaCl, 0.1% Triton X-100, 0.1% Nonidet P-40, 4 mmol/L EDTA, 50 mmol/L NaF, 0.1 mmol/L NaV, 1 mmol/L DTT, and 10 mg/mL each of the protease inhibitors antipain, leupeptin, pepstatin A, chymostatin, and 50 mg/mL phenylmethylsulfonyl fluoride (PMSF). Protein concentration of cell extracts was determined (Bio-Rad), and aliquots containing equal amounts of protein were separated by SDS-PAGE and then transferred to nitrocellulose membrane. Filters were then processed and probed with appropriate antibodies to detect PARP. Protein-antibody complexes were visualized by enhanced chemiluminescence.

Animals and xenograft murine model. *In vivo* studies were carried out in 4- to 6-week-old male beige, nude, *Xid* mice obtained from Harlan Sprague-Dawley, with animals maintained under pathogen-free conditions. Mice received a single i.p. injection of 1.3 to 1.6 × 10^7 REN cells in a volume of 1 mL serum-free media, and Bortezomib therapy was initiated 3 days later at the dosage described above. Preliminary experiments revealed that mice injected with 1.3 to 2.0 × 10^7 cells developed small i.p. tumor masses within 15 days following tumor cell injection and progressed to multiple small mesenteric tumor nodules by day 22. By day 28, 75% of injected mice contained large peri-pancreatic tumors (1.0-1.5 cm) with multiple mesenteric nodules, bloody ascites, and diaphragmatic tumors. By day 35, more than 95% of the animals present very large, bulky peri-pancreatic tumors (2.0-2.5 cm), numerous large mesenteric nodules, large amounts of bloody ascites, and bulky diaphragmatic involvement. Mean survival in untreated animals in these previous studies was 68 days (range, 63-74 days; ref. 25). For scoring purposes in this study, we defined diaphragmatic involvement at the time of sacrifice (day 30 after tumor cell injection) as "none" if no tumoral involvement was macroscopically detectable, "mild" if only few tumoral nodules were detectable and covered less than one-third of the surface of the diaphragm, "moderate" if tumoral nodules accounted for one-third to two thirds of the surface, and "massive" if dissemination of tumoral masses covered more than two-thirds of the surface.

All animal experiments were done in accordance with institutional animal committee guidelines. Mice were maintained and handled under aseptic conditions, and animals were allowed access to food and water ad libitum. The study was repeated.

Statistics. *In vitro* data were expressed as mean ± SD of at least three independent experiments. Statistical differences were evaluated by Student's *t* test, with significance threshold of at least 95% confidence or higher. All statistical tests were two sided. For statistical analysis of the *in vivo* results, we assessed drug effectiveness by three measures taken at the termination of each trial: (*a*) tumor weight, (*b*) ascite volume, and (*c*) the extent of diaphragm involvement, classified as none, mild, moderate, or massive as described above.

We assessed ascite volume on a dichotomous scale, assigning volumes of traces or greater as positive and volumes of 0 as negative. For parametric analyses, we used log-transformed values of tumor weight; to address zero values, 0.01 mg/kg was added to each tumor-weight value before the transformation. We used the Kruskal-Wallis test of equality of populations to assess for differences among the ranked values of diaphragm involvement. Because there were no statistically significant differences among the two trials in measures (by treatment class) of ascite or diaphragm involvement, we assessed treatment differences of these measures within and across trials; because of a significant difference in tumor weight between trials, we did within-trial analyses only for this measure.

Results

NF-κB is an intrinsic survival factor in MMe cells and in HMC when exposed to asbestos fibers. To determine the state of NF-κB activation in HMC, DNA binding assay was conducted; DNA binding was barely detectable in HMC, whereas it was constitutive in MMe cells MMP, MMB, and REN (Fig. 1A). HGF is one of the most important growth factors involved in mesothelial transformation, mainly upon autocrine loop (26); thus, we assessed the effect of HGF exposure on NF-κB in HMC cells. In contrast to what previously observed in epithelial MLP29 cells (23), NF-κB DNA binding was not increased by HGF, suggesting a different, cell type–dependent mechanism of NF-κB activation. Cell treatment with Bay 11-7082, a known inhibitor of IκB-α phosphorylation, resulted in the substantial reduction of NF-κB activity in MMe cells (Fig. 1A). On the contrary, inhibitors of tyrosine kinase activity (Genistein), of Src (PP2), of Erk2 (PD98059), of PI3K/Akt (wortmannin), and of p38 (SB203580) did not affect NF-κB DNA binding in any cell type tested (Fig. 1B).

The intracellular localization of NF-κB complexes was analyzed in MMe cells (REN and MMP) following 2 h stimulation with TNF-α (4 ng/mL) or treatment with the exportin-1 inhibitor LMB (1 ng/mL) by HCA of the fluorescence signal associated to $p65^{RelA}$ immunostaining. As shown in Fig. 1C, in untreated REN and MMP cells, the nuclear/cytoplasmic shuttling rate of $p65^{RelA}$ was prevalently found shifted toward the cytoplasm. Both TNF-α and LMB altered the nuclear/cytoplasmic distribution, inducing NF-κB nuclear accumulation and revealing that these complexes undergo dynamic nuclear-cytoplasmic shuttling.

As expected, exposure of HMC to amosite fibers induced NF-κB DNA binding, whereas transfection of SV40, a well-known carcinogen cofactor of mesothelioma (27), did not affect NF-κB

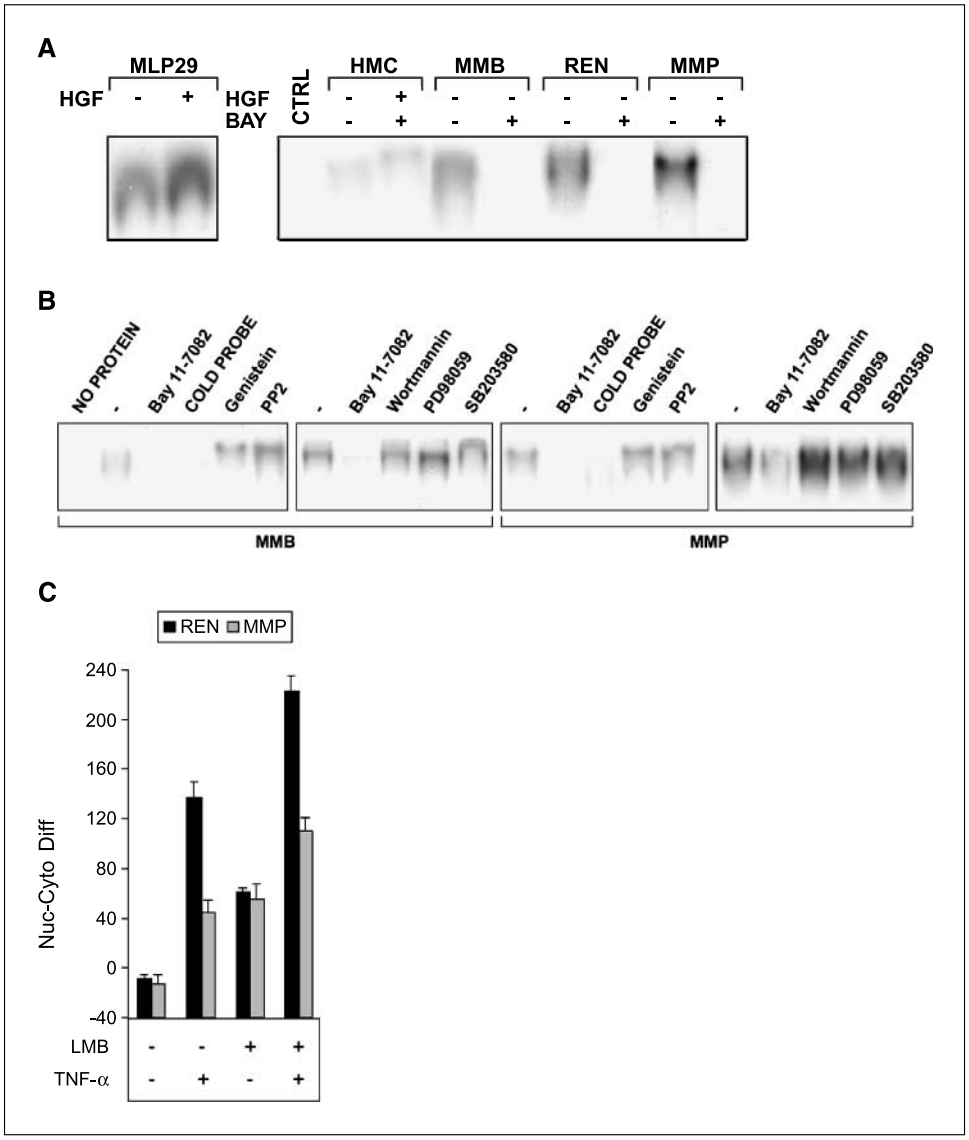

Fig. 1. NF-κB activity in mesothelial and mesothelioma cells. *A,* EMSA analysis of mesothelial (*HMC*) and mesothelioma (*MMB, REN*, and *MMP*) cells in the presence of HGF and Bay 11-7082. Murine liver progenitor cells (*MLP29*) were as controls of HGF responsiveness. CTRL, EMSA in the absence of protein. *B,* EMSA analysis on nuclear extracts from the indicated cells as described in Materials and Methods. Before lysis, cells were treated with the indicated panel of inhibitors of intracellular activities and effectors. The compounds were inhibitors of: tyrosine kinase activity (*Genistein*), Src (*PP2*), Erk1/2 (*PD98059*), PI3K (*Wortmannin*), and p38 (*SB203580*). CTRL, EMSA in the absence of protein. –, no treatment. COLD PROBE, incubated with unlabeled oligonucleotide probe. *C,* REN and MMP cells were treated with 1 ng/mL LMB or stimulated with 4 ng/mL TNF-α, alone or in combination for 2 h. Cells were fixed, immunostained with anti – NF-κB ($p65^{RelA}$) antibody, and counterstained with DAPI. NF-κB nuclear translocation index was measured by HCA and expressed as the difference between nuclear and cytoplasmic NF-κB – related fluorescence intensity. Columns, means of at least three replicates; bars, SD.

activity in HMC nor MMe cells (data not shown). Treatment of HMC with 5 μmol/L Bay 11-7082 was not cytotoxic; however, as previously reported (20), HMC exposure to a low density of amosite fibers (2.5 $\mu g/cm^2$) induced cytotoxicity potentiated by 5 μmol/L Bay 11-7082 ($P = 0.0001$). In contrast, Bay 11-7082 alone exerted cytotoxicity in both REN and MMP cells (Fig. 2A). We have previously shown that HMC transfected with SV40 DNA and exposed to amosite fibers according to the long-term exposure undergo cell transformation and foci formation (20). Over the 60-day time span required for full cell transformation, transformed HMC became progressively insensitive to amosite cytotoxic effect. Bay 11-7082 significantly increased their sensitivity to amosite, consistent with a role for NF-κB signaling in asbestos-dependent transformation of HMC (Fig. 2A). The same transformed cells derived from foci displayed NF-κB in activated, phosphorylated form and NF-κB DNA binding activity (Fig. 2B). We conclude that NF-κB activity, elicited by amosite in HMC, is constitutive in MMe cells, providing survival signaling both in normal and transformed HMC, analogously to MMe cells.

Bortezomib inhibits NF-κB activity in MMe cells. Based on the observation that NF-κB is constitutively activated in MMe cell lines, we tested the effects on these cells of the proteasome inhibitor Bortezomib that inhibits NF-κB activity by preventing IκB degradation in different cancer models (16). As assessed by EMSA, 24 h exposure of REN cells to either 25 or 100 nmol/L Bortezomib decreased NF-κB DNA binding activity in a dose-dependent manner (Fig. 3A).

The effect of Bortezomib on NF-κB activity by nuclear translocation analysis was conducted. In REN and MMP cells, a prevalent cytoplasmic localization was observed; however, following 1 h of TNF-α stimulation, NF-κB massively relocalized to the nucleus in both cell types, consistently with its activation (Fig. 3B and C). Cytokine-induced nuclear translocation was almost completely prevented by pretreatment with both the known irreversible inhibitor of IκB-α phosphorylation Bay 11-7082 or Bortezomib. Both Bortezomib and Bay 11-7082 as single agents induced a slight increase of NF-κB nuclear translocation signal in both cell lines. Visual inspection of fields acquired by HCA suggested that this effect could be due, for Bortezomib, to cell-cycle block induction, resulting in the accumulation of mitotic cells (in particular for REN), which have no nuclear envelope, together with the induction of

apoptosis. Bay 11-7082 was also found to induce cell death (Fig. 2A), associated with altered spreading and actin cytoskeleton remodeling, as already reported in other cellular models (28). Finally, a slight increase in the mean NF-κB translocation value was observed in the overall cell population; this could be due to the sensitivity of the nuclear translocation parameter, which can be affected by morphologic alterations induced by treatment, such as mitosis, cell spreading, apoptosis, or cytotoxicity calculated by imaging approach.

Taking into account those morphologic alterations, both Bortezomib and Bay 11-7082 alone did not significantly modify the NF-κB nuclear translocation value in basal conditions. However, the two compounds efficiently inhibited cytokine-induced NF-κB nuclear translocation and induced cytotoxicity both in basal conditions (MMe) and when exposed to asbestos fibers (HMC and MMe).

These results confirm that Bortezomib significantly reduces NF-κB nuclear translocation and, in turn, its DNA binding activity at the same extent of Bay-117082, suggesting a specific NF-κB targeting.

Bortezomib induces MMe cell death, G_2-M cell cycle blockade, and apoptosis. The cytotoxic effect of Bortezomib in MMe cells was determined by MTT assay (29). Exposure to Bortezomib for 24 h resulted in a remarkable dose-dependent cytotoxic effect. The estimated EC_{50} values were 18.6 nmol/L (SD, 3.6) and 51.4 nmol/L (SD, 18.8) for REN and MMP cells, respectively

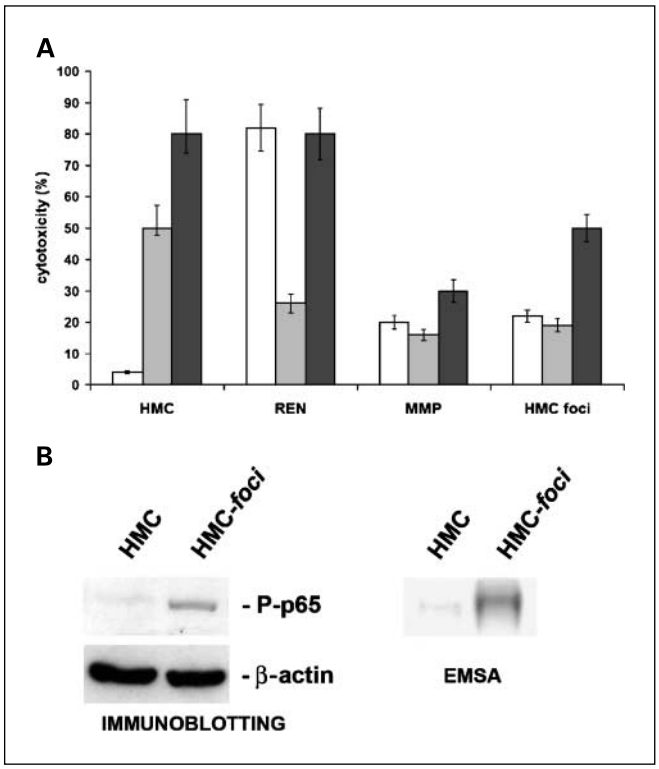

Fig. 2. Activated form of NF-κB exerts a prolonged cell survival after amosite exposure. *A,* MTT assay on the indicated cells, treated with 5 μmol/L Bay 11-7082 (*white columns*), exposed to 2.5 μg/cm^2 amosite fibers alone (*gray columns*), or in the presence of Bay 11-7082 (*black columns*). Columns, means of at least three replicates; bars, SD. *B,* immunoblotting and EMSA on mesothelial cells (*HMC*) and on mesothelial cells derived from foci (*HMC-foci*), upon long-term exposure to amosite (see Materials and Methods). P-p65, phosphorylated (activated) form of p65^{relA} NF-κB subunit. β-actin, loading control.

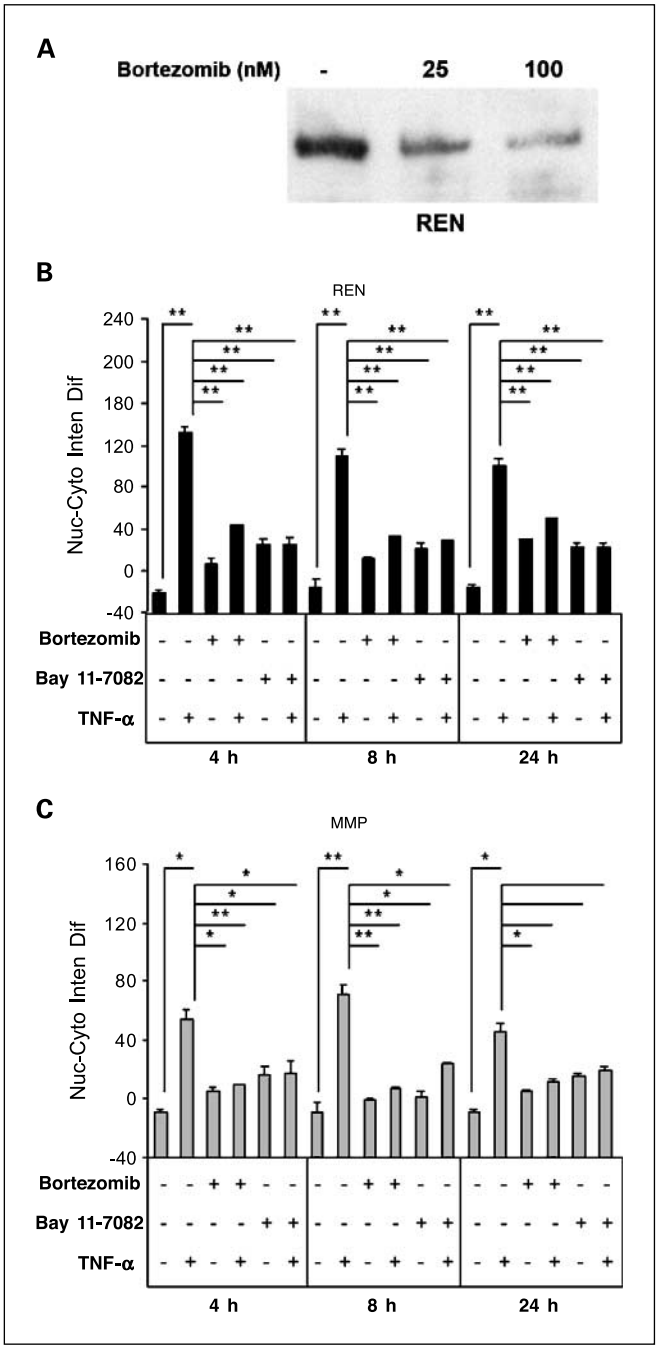

Fig. 3. Effects of Bortezomib on NF-κB binding activity and cytokine-induced NF-κB nuclear translocation in MMe cells. *A,* NF-κB DNA binding activity tested by EMSA upon treatment of REN cells with Bortezomib at 25 and 100 nmol/L for 24 h. *B* and *C,* nuclear translocation analysis. REN (*B*) and MMP (*C*) cells were treated with 1 μmol/L Bortezomib or 50 μmol/L Bay 11-7082 for 4, 8, or 24 h and then stimulated or not for the last hour with 4 ng/mL TNF-α. Cells were fixed, immunostained with anti – NF-κB (p65^{RelA}) antibody, and counterstained with DAPI. NF-κB nuclear translocation index was measured by HCA and expressed as the difference between nuclear and cytoplasmic NF-κB – related fluorescence intensity. Columns, means of at least three replicates; bars, SD. *, $P < 0.05$; **, $P < 0.01$.

(data not shown). In contrast, HMC viability was not affected by Bortezomib treatment.

The effects of Bortezomib on cell cycle and apoptosis induction were tested in REN and MMP cells by HCA. MMe

cells were exposed to increasing doses of Bortezomib (ranging from 3 to 800 nmol/L) for three time points (24, 48, and 72 h). For each concentration, the percentage of remaining cells with respect to untreated controls, together with the percentages of positively stained cells for cyclin B1, BrdUrd, and active caspase-3 were calculated and reported in dose-response curves. Interestingly, the concentrations at which Bortezomib exerts its antiproliferative activity were found to be consistent with the therapeutic dose ranges (30).

In REN cells, Bortezomib inhibited cell growth at 24 h by inducing a G_2-M cell cycle block, with an estimated EC_{50} of 33 nmol/L (Fig. 4A, *left*). This was confirmed by the accumulation of cyclin B1 – positive cells and overall cell number decrease (EC_{50} of 38 nmol/L). In parallel, a decrease in cells engaged in active S-phase (BrdUrd, EC_{50} = 57 nmol/L) and relevant apoptosis induction (active caspase-3, EC_{50} = 65 nmol/L) were also evident. At 48 h, either cyclin B1 – stained cells and the overall cell number dramatically decreased at doses above 50 nmol/L, in parallel with an increase of apoptotic cells. After 72 h of treatment, HCA profiles of REN cells indicated a massive cell loss at Bortezomib doses above 25 nmol/L, and the few remaining cells were apoptotic. The biphasic behavior of cyclin B1 curves at 48 and 72 h (first increasing and decreasing at higher doses) indicates that cells progressively undergo apoptotic cell death from an early cycle block in the G_2-M phase. These data indicate that Bortezomib antiproliferative activity on REN cells mainly occurs upon the induction of the G_2-M block followed by massive apoptosis.

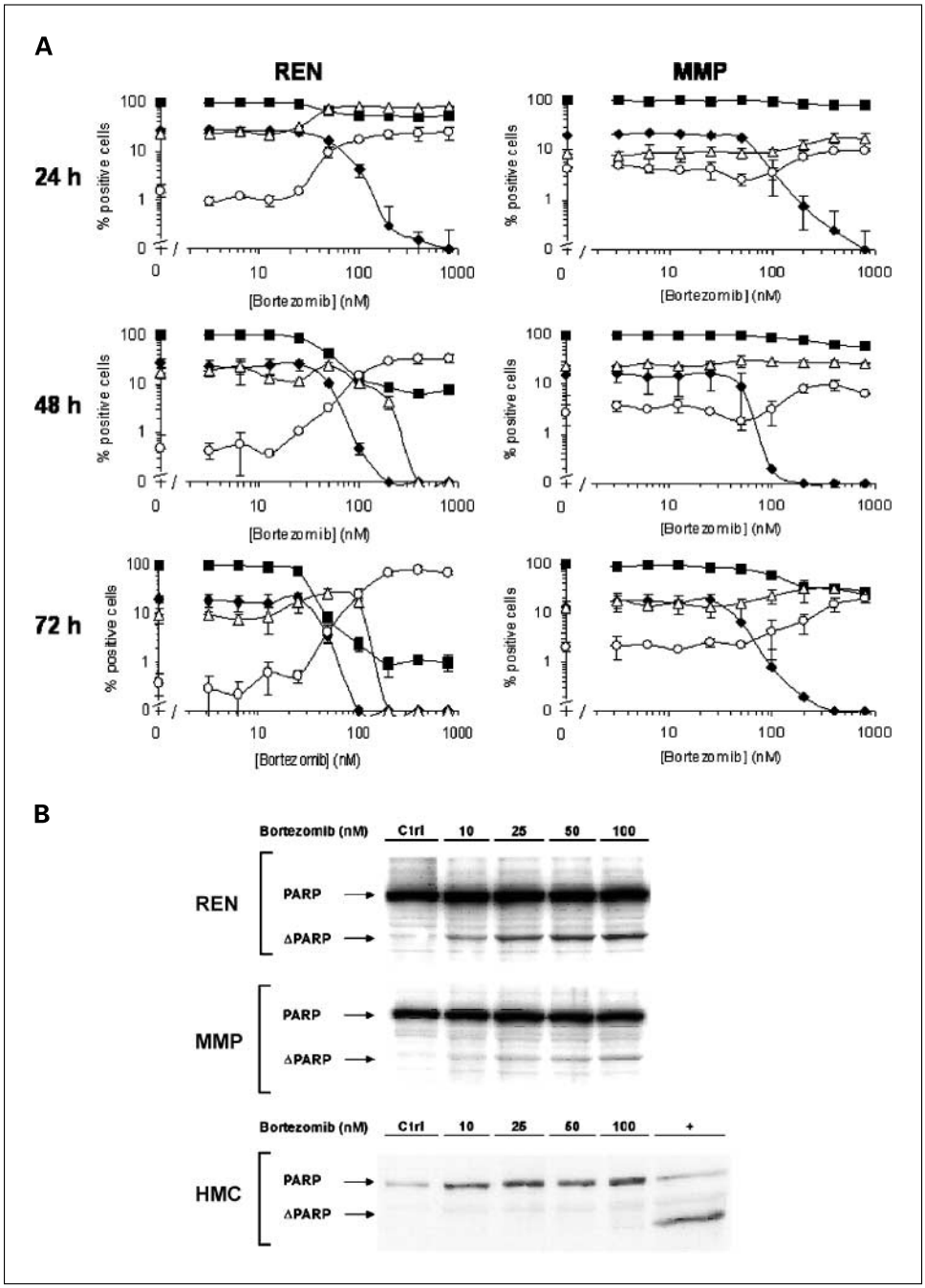

Fig. 4. Bortezomib induces cell cycle block and apoptosis in REN and MMP cells. *A,* REN and MMP cells were treated with increasing concentrations of Bortezomib (ranging from 3 to 800 nmol/L) for 24, 48, or 72 h and then processed for immunofluorescence and HCA. For each concentration, the number of cells scored in 10 fields was reported as percentage with respect to untreated controls (■) counted on the basis of their nuclear DAPI fluorescence. The percentages of cells positively stained for BrdUrd incorporation (♦), cyclin B1 (△), and active caspase-3 (○) were also calculated. Points, means of at least three replicates; bars, SD. *B,* immunoblotting analysis on REN, MMP, and HMC cell lysates after 24 h exposure to 10 to 100 nmol/L Bortezomib. ΔPARP, 89-kDa cleaved fragment.

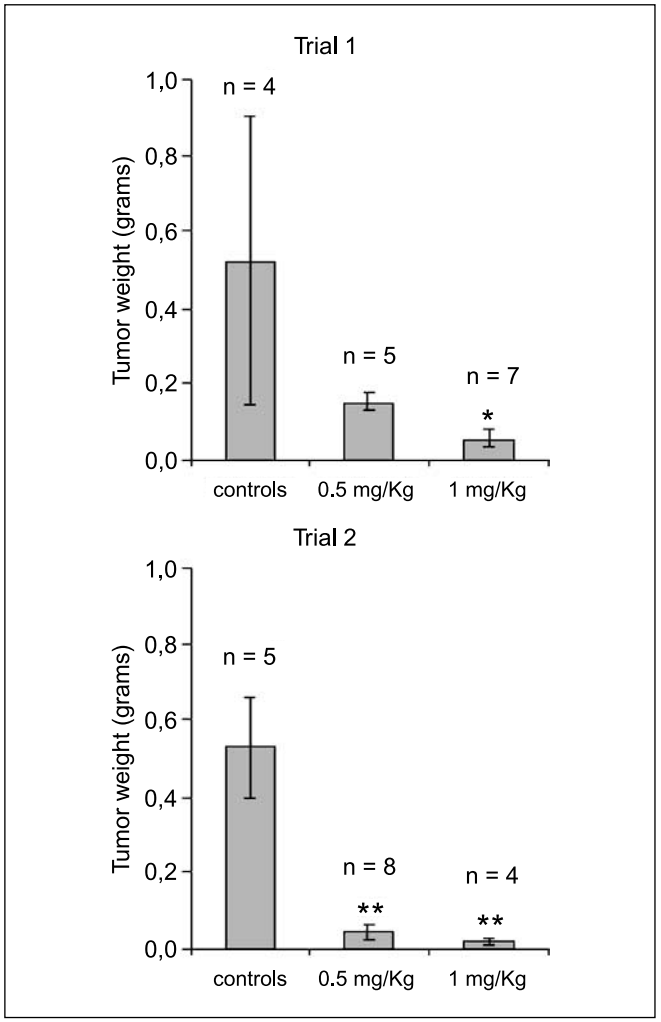

Fig. 5. Antitumor activity of Bortezomib in the mesothelioma xenograft murine model. About 1.3 to 1.6 $\times$ 10^7 REN cells were injected i.p. in nude *xid* mice; treatment with Bortezomib was started 3 days after tumor inoculation to allow engraftment. Doses evaluated were 0.5 and 1 mg/kg/day, given twice a week on a Monday/Thursday schedule for 4 wks. Control untreated animals received single i.p. bolus injection of vehicle alone. Tumor weight at the time of sacrifice (day 30) is indicated. Columns, means for the two different trials done; bars, SD. *, $P < 0.05$; **, $P < 0.01$.

In MMP cells, despite the decrease in BrdUrd incorporation (EC_{50} = 71 nmol/L) and the induction of apoptosis (EC_{50} = 200 nmol/L) at 24 h, the cell number did not change significantly (Fig. 4A, *right*). Moreover, only a slight accumulation of G_2-M cells was observed at higher doses. After 48 and 72 h, these perturbation trends of all parameters were emphasized, although a significant cell number decrease was achieved only at 72 h (EC_{50} = 100 nmol/L). This indicates that Bortezomib inhibited cell proliferation, as confirmed by a decrease in BrdUrd incorporation, albeit with less efficacy with respect to REN cells. Cell-cycle and apoptotic effects on both cell lines were confirmed by flow cytometry analysis of DNA content, done in parallel (data not shown).

To further assess the proapoptotic activity of Bortezomib, Western blot analysis of PARP cleavage was done on cell lysates from REN, MMP, and HMC cells treated with 10 to 100 nmol/L of Bortezomib for 24 h. As shown in Fig. 4B, cleavage of PARP occurred in REN and MMP cells starting at the dosage of 10 and 25 nmol/L, respectively. This confirmed the HCA profiles of apoptosis induction. PARP cleavage was undetectable in HMC cells.

Bortezomib inhibits tumor growth in an* in vivo *model of malignant mesothelioma. To determine if exposure to Bortezomib could inhibit MMe tumor growth *in vivo*, xenografts of REN cells were generated in nude *xid* mice. REN cells were injected i.p. into mice and allowed to engraft for 3 days. Mice, randomly distributed into groups of four to eight animals, were then treated with Bortezomib at doses of 0.5 and 1.0 mg/kg, given by i.p. bolus injection twice weekly for 4 weeks. Control animals received the same schedule of vehicle (saline) alone. Mice were sacrificed on day 30 after tumor cell injection for measurement of ascites volume, removal and weighing of all tumor foci, and notation of gross tumor involvement of the diaphragm for each animal. Two *in vivo* trials were carried out, and Bortezomib mediated inhibition of tumor growth (Fig. 5). In particular, at 1 mg/kg Bortezomib, a significant inhibition of tumor weight was noted in both trials ($P < 0.05$ in trial 1; $P < 0.01$ in trial 2). In trial 2, a significant inhibition of tumor growth was also observed at the lower dose of 0.5 mg/kg ($P < 0.01$).

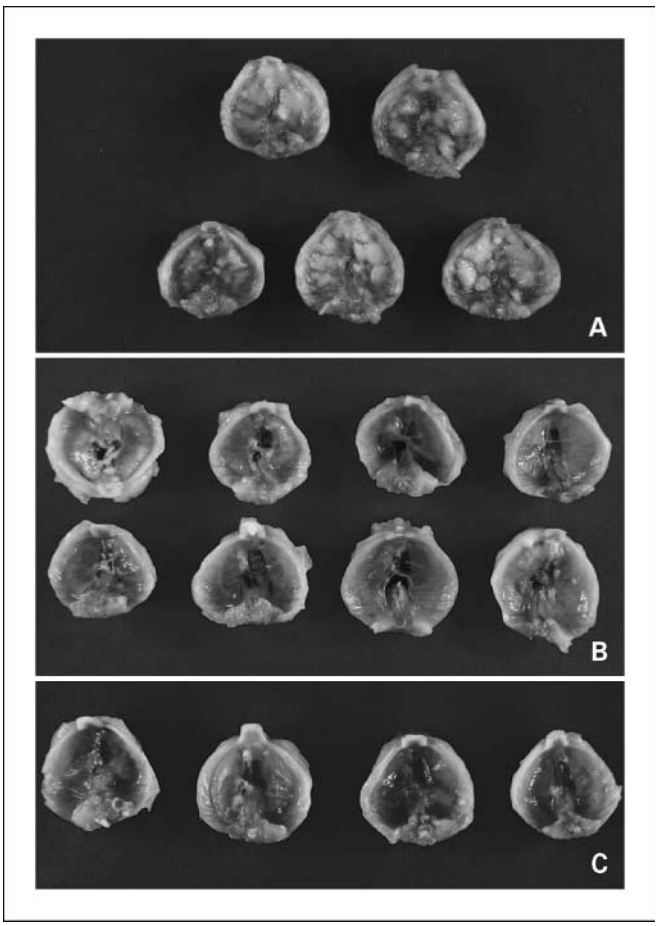

Fig. 6. Inhibition of diaphragmatic tumor growth by Bortezomib in REN tumor-bearing mice. Representative pictures from trial 2. At the time of sacrifice, diaphragm involvement was evaluated by resection in each animal. Underside of diaphragms are shown. *A,* in untreated (control) mice, large, bulky tumor are evident. *B,* in the 0.5-mg/kg group, few tumor nodules are seen. *C,* no gross evidence of tumor involvement in the 1-mg/kg group.

Table 1. *In vivo* evaluation of the ability of Bortezomib to prevent diaphragmatic tumor formation in a model of malignant mesothelioma

Diaphragm involvement	Bortezomib dose		
	Control (0 mg/kg)	0.5 mg/kg	1.0 mg/kg
Massive	5/9	0/13	0/11
Moderate	1/9	0/13	0/11
Mild	2/9	2/13	0/11
None	1/9	11/13	11/11

NOTE: About 1.3 to 1.6 $\times$ 10^7 REN cells were injected i.p. in nude *xid* mice; 3 d after tumor inoculation treatment with Bortezomib at dosages of 0.5 or 1.0 mg/kg/day was started. Drug was given i.p. twice weekly for 4 wk. Control animals received single i.p. bolus injection of vehicle alone. Two different trials using the same experimental conditions were done. The table summarizes the antitumor activity of Bortezomib as assessed by the extent of diaphragm involvement (classified as none, mild, moderate, or massive; see Materials and Methods).

Based on the recorded volume of ascites, these data were assessed on a dichotomous scale, assigning trace or greater volumes as positive and zero volumes as negative. Analysis across trials showed that 88.5% of control animals presented positive for ascites, compared with 46.0% in the 0.5-mg/kg group and 17.4% in the 1-mg/kg group ($\chi^2 = 18.06$, $P < 0.0001$).

Finally, treatment with Bortezomib dramatically reduced diaphragm involvement, with none of the 1-mg/kg dose group presenting any involvement and 15.4% of the 0.5-mg/kg dose group showing mild involvement only. In the control group, 55.5% of the mice presented with massive, 33.3% with moderate/mild, and 11.1% with no apparent involvement (χ^2 = 24.50, P < 0.0001; Table 1). Figure 6 shows the abdominal surface of the diaphragms from all animals in trial 2. Finally, only Bortezomib-treated animals seemed healthy throughout each of the studies, and no significant weight loss was noted in any drug-treated mice.

Discussion

This report provides evidence supporting a role for NF-κB activation and nuclear translocation in inducing resistance to cell death of HMC and MMe cells exposed to asbestos fibers and contributing to HMC transformation. Moreover, inhibition of NF-κB constitutive activation in MMe cells by Bortezomib resulted in *in vitro* cytotoxicity along with apoptosis and *in vivo* tumor regression.

NF-κB is well known to be activated upon exposure to a variety of extracellular stimuli as oxidative stress, hypoxia, inflammatory cytokines, and others (5). The presence of these factors in the tumor microenvironment is consistent with the finding of a constitutive NF-κB activation in mesothelioma tumor cells.

Our results provide further evidence that asbestos fibers, the main established cause of MMe, cause the translocation of NF-κB p65 subunit into the nucleus and increase NF-κB DNA binding activity in pleural mesothelial cells, in accordance with a number of previous studies (31–39). Interestingly, a recent work shows that in HMCs, TNF-α induces cell survival, and resistance to asbestos induced cytotoxicity via NF-κB, indicating a critical role for this transcriptional factor in cells exposed to asbestos (40). Our paper is in accordance with these data and is the first evidence of the role of NF-κB as a survival factor in MMe cells.

SV40 infection has been recently considered as a relevant co-causative agent of MMe (20, 41–45) by activating several survival signaling pathways (26, 46–48).

According to our previous study (20), we exploited an *in vitro* model of SV40/fibers combined transforming process to verify if NF-κB can contribute to a fully transformed phenotype of HMC, via progressive resistance to asbestos fibers. Our results clearly show that NF-κB acts as an additional survival factor for HMC exposed to asbestos, leading to the transformation and for MMe cells in basal conditions. These results provide the evidence that NF-κB plays a role in MMe oncogenesis as in many other human tumors (4).

PI3K/Akt signaling pathway has been implicated in NF-κB activation (reviewed in ref. 49), and more recently, it has been shown that NF-κB is activated independently by Akt (50), whereas the pathway leading to NF-κB activation has been linked to cell type variations (51). We show here that both in HMC and in MMe cells, NF-κB activity is not related to PI3K/Akt signaling. Nevertheless, our results do not clarify which signaling pathway is responsible for NF-κB activity in all cells investigated. Given that neither mitogen-activated protein kinase inhibition (Erk1 and 2 or p38) nor wortmannin affects NF-κB activity, in contrast to what is observed in other cell types (52), the underlying pathway activating NF-κB in these cells is currently under investigation.

Platelet-derived growth factor (PDGF) and epidermal growth factor (EGF) are candidates for NF-κB activation, but our findings show that neither the general tyrosine kinase inhibitor (genistein) nor the specific Src inhibitor (PP2) affects NF-κB activity. In contrast, we provided evidence that HGF leads to NF-κB activation in epithelial MLP29 cells, albeit neither related to survival nor to PI3K/Akt activity (23). This does not occur in HMC or MMe cells, where HGF exerts its antiapoptotic effect independently to NF-κB activation.

Cells derived from the foci of SV40-HMC cultures are significantly more resistant to asbestos than HMC, whereas Bay 11-7082 restores sensitivity to amosite more significantly in HMC than in foci cells. Likewise, although sensitivity to asbestos of MMe cells was similarly low, despite the presence or absence of SV40, Bay 11-7082 was more effective in SV40-negative REN than in SV40-positive MMP. The additive survival effects due to SV40-dependent Akt activation, as reported for other tumors (53), and the higher basal NF-κB activity were possibly responsible for these discrepancies. Altogether, our results indicate that NF-κB plays an additional role on the induction of cytotoxicity resistance to asbestos in HMC on top of the parallel well-known effect on tumor progression of SV40-dependent Akt activation (54).

Our results confirm that the NF-κB inhibitor Bay 11-7082 leads to specific MMe cells death, whereas NF-κB inhibition has been recently discussed as a novel target for the treatment of human tumors (55, 56). This prompted us to hypothesize the use of compounds aimed at NF-κB inhibition as novel tailored targeted therapy for MMe and we verified if Bortezomib inhibition of NF-κB could induce apoptotic cell death in this neoplasm. Although the proteasome-inhibitory activity of

Bortezomib may well interfere with many other apoptotic signaling pathways (53), we focused on NF-κB inhibition as a relevant therapeutic target in MMe cells.

NF-κB constitutive activation in MMe induces signals leading to cell proliferation and inhibition of apoptosis of these tumor cells. EMSA shows that in MMe cells, NF-κB is constitutively bound to DNA, although immunostaining of $p65^{RelA}$ apparently indicates that in untreated cells, NF-κB complexes primarily localize to the cytoplasm. However, data from EMSA and NF-κB translocation are only apparently in conflict: treatment with the exportin-1 inhibitor LMB induces NF-κB nuclear accumulation, revealing that these complexes undergo dynamic nuclear-cytoplasmic shuttling, as previously reported (57). In steady state, the majority of NF-κB complexes localizes to the cytoplasm bound to IκB-α as result of a shift in the dynamic equilibrium toward the nuclear export. The effect of Bortezomib on NF-κB nuclear translocation was evaluated in REN and MMP cells by HCA; we found that, upon cytokine stimulation conditions, which mimic the *in vivo* tumor microenvironment (4), Bortezomib efficiently inhibits NF-κB nuclear translocation. We used TNF-α to induce NF-κB activation in REN and MMP cells. Treatment of MMe cells with Bay 11-7082, a specific IκB-α stabilizer, also resulted in the inhibition of cytokine-induced NF-κB nuclear translocation, as expected. All in all, our data indicate that in MMe cells (but not in HMC), NF-κB dynamically shuttles across the nuclear envelope, and our data confirm that, despite a prevalent cytoplasmic localization in steady state, a subset of NF-κB complexes actually localizes to the nucleus and is responsible for the constitutive basal activation of NF-κB target genes.

Bortezomib induces apoptosis in MMe cells, as evidenced by PARP cleavage that correlates with a marked reduction in NF-κB activity and cell cycle arrest (15, 58). Although our *in vitro* results clearly suggest that Bortezomib exerts its effects on MMe cells via NF-κB, one cannot exclude the fact that also the modulation of further survival pathways may be involved.

Our *in vivo* results were generated in a model that mimics some clinical features of mesothelioma, including the formation of malignant effusion and progressive i.p. tumor spread. The ability of Bortezomib to abrogate the spread of the tumor to the diaphragmatic surface as well as the formation of malignant effusions, along with its safety, supports the use of Bortezomib in the treatment of MMe and suggests a role for the administration of this agent for therapeutic purposes. The role of NF-κB in conferring HMC cellular resistance to apoptosis and MMe carcinogenesis might suggest the hypothesis that Bortezomib administration could be pursued as a potential chemopreventive treatment for people exposed to asbestos fibers. On the basis of these preclinical findings, a phase II clinical trial with Bortezomib as a single agent for patients with relapsed MMe is currently ongoing across Europe along with a European Organization for Research and Treatment of Cancer phase II trial incorporating Bortezomib and cisplatin combination therapy planned.

Acknowledgments

In memory of Paul Calabresi.

We thank the Italian Group for the Study and Therapy of Malignant Mesothelioma (G.I.Me, Italy) for the logistic support. We thank Steven E. Reinert for the statistical analysis and Dr. Vittorio Rosti for his comments on the manuscript.

References

1. Peto J, Decarli A, La Vecchia C, Levi F, Negri E. The European mesothelioma epidemic. Br J Cancer 1999; 79:666–72.
2. Fisher SG, Weber L, Carbone M. Cancer risk associated with simian virus 40 contaminated polio vaccine. Anticancer Res 1999;19:2173–80.
3. Zucali PA, Giaccone G. Biology and management of malignant pleural mesothelioma. Eur J Cancer 2006; 42:2706–14.
4. Baldwin AS. Control of oncogenesis and cancer therapy resistance by the transcription factor NF-κB. J Clin Invest 2001;107:241–6.
5. Roff M, Thompson J, Rodriguez MS, et al. Role of IκBα ubiquitination in signal-induced activation of NFκB *in vivo*. J Biol Chem 1996;271:7844–50.
6. Bours V, Burd PR, Brown K, et al. A novel mitogen-inducible gene product related to p50/p105–NF-κB participates in transactivation through a κB site. Mol Cell Biol 1992;12:685–95.
7. Lind DS, Hochwald SN, Malaty J, et al. Nuclear factor-κB is upregulated in colorectal cancer. Surgery 2001;130:363–9.
8. Mukhopadhyay T, Roth JA, Maxwell SA. Altered expression of the p50 subunit of the NF-κB transcription factor complex in non–small cell lung carcinoma. Oncogene 1995;11:999–1003.
9. Nakshatri H, Bhat-Nakshatri P, Martin DA, Goulet RJ, Jr., Sledge GW, Jr. Constitutive activation of NF-κB during progression of breast cancer to hormone-independent growth. Mol Cell Biol 1997;17:3629–39.
10. Ondrey FG, Dong G, Sunwoo J, et al. Constitutive activation of transcription factors NF-(κ)B, AP-1, and NF-IL6 in human head and neck squamous cell carcinoma cell lines that express pro-inflammatory and pro-angiogenic cytokines. Mol Carcinog 1999;26: 119–29.
11. Sovak MA, Bellas RE, Kim DW, et al. Aberrant nuclear factor-κB/Rel expression and the pathogenesis of breast cancer. J Clin Invest 1997;100:2952–60.
12. Wang W, Abbruzzese JL, Evans DB, Larry L, Cleary KR, Chiao PJ. The nuclear factor-κB RelA transcription factor is constitutively activated in human pancreatic adenocarcinoma cells. Clin Cancer Res 1999;5:119–27.
13. Cusack JC, Liu R, Baldwin AS. NF-κB and chemoresistance: potentiation of cancer drugs via inhibition of NF-κB. Drug Resist Updat 1999;2:271–3.
14. Russo SM, Tepper JE, Baldwin AS, Jr., et al. Enhancement of radiosensitivity by proteasome inhibition: implications for a role of NF-κB. Int J Radiat Oncol Biol Phys 2001;50:183–93.
15. Adams J, Palombella VJ, Sausville EA, et al. Proteasome inhibitors: a novel class of potent and effective antitumor agents. Cancer Res 1999;59:2615–22.
16. Lenz HJ. Clinical update: proteasome inhibitors in solid tumors. Cancer Treat Rev 2003;29 Suppl 1:41–8.
17. Borczuk AC, Cappellini GC, Kim HK, Hesdorffer M, Taub RN, Powell CA. Molecular profiling of malignant peritoneal mesothelioma identifies the ubiquitin-proteasome pathway as a therapeutic target in poor prognosis tumors. Oncogene 2007;26:610–7.
18. Sun X, Gulyas M, Hjerpe A, Dobra K. Proteasome inhibitor PSI induces apoptosis in human mesothelioma cells. Cancer Lett 2006;232:161–9.
19. Smythe WR, Kaiser LR, Hwang HC, et al. Successful adenovirus-mediated gene transfer in an *in vivo* model of human malignant mesothelioma. Ann Thorac Surg 1994;57:1395–401.
20. Cacciotti P, Barbone D, Porta C, et al. SV40-dependent AKT activity drives mesothelial cell transformation after asbestos exposure. Cancer Res 2005;65:5256–62.
21. Gasparri F, Cappella P, Galvani A. Multiparametric cell cycle analysis by automated microscopy. J Biomol Screen 2006;11:586–98.
22. Cohen GM. Caspases: the executioners of apoptosis. Biochem J 1997;326:1–16.
23. Muller M, Morotti A, Ponzetto C. Activation of NF-κB is essential for hepatocyte growth factor-mediated proliferation and tubulogenesis. Mol Cell Biol 2002;22:1060–72.
24. Ding GJ, Fischer PA, Boltz RC, et al. Characterization and quantitation of NF-κB nuclear translocation induced by interleukin-1 and tumor necrosis factor-α. Development and use of a high capacity fluorescence cytometric system. J Biol Chem 1998; 273:28897–905.
25. Nici L, Monfils B, Calabresi P. The effects of taurolidine, a novel antineoplastic agent, on human malignant mesothelioma. Clin Cancer Res 2004;10: 7655–61.
26. Cacciotti P, Libener R, Betta P, et al. SV40 replication in human mesothelial cells induces HGF/Met receptor activation: a model for viral-related carcinogenesis of human malignant mesothelioma. Proc Natl Acad Sci U S A 2001;98:12032–7.
27. Carbone M, Pass HI, Miele L, Bocchetta M. New developments about the association of SV40 with human mesothelioma. Oncogene 2003;22:5173–80.
28. Hammar EB, Irminger JC, Rickenbach K, et al. Activation of NF-κB by extracellular matrix is involved in spreading and glucose-stimulated insulin secretion of pancreatic beta cells. J Biol Chem 2005;280: 30630–7.
29. Mosmann T. Rapid colorimetric assay for cellular growth and survival: application to proliferation and cytotoxicity assays. J Immunol Methods 1983;65: 55–63.

30. Ryan DP, O'Neil BH, Supko JG, et al. A Phase I study of bortezomib plus irinotecan in patients with advanced solid tumors. Cancer 2006;107:2688–97.

31. Janssen YM, Barchowsky A, Treadwell M, Driscoll KE, Mossman BT. Asbestos induces nuclear factor κB (NF-κB) DNA-binding activity and NF-κB–dependent gene expression in tracheal epithelial cells. Proc Natl Acad Sci U S A 1995;92:8458–62.

32. Faux SP, Howden PJ. Possible role of lipid peroxidation in the induction of NF-κB and AP-1 in RFL-6 cells by crocidolite asbestos: evidence following protection by vitamin E. Environ Health Perspect 1997;105 Suppl 5:1127–30.

33. Janssen YM, Driscoll KE, Howard B, et al. Asbestos causes translocation of p65 protein and increases NF-κB DNA binding activity in rat lung epithelial and pleural mesothelial cells. Am J Pathol 1997;151:389–401.

34. Mossman BT, Faux S, Janssen Y, et al. Cell signaling pathways elicited by asbestos. Environ Health Perspect 1997;105S:1121–5.

35. Cheng N, Shi X, Ye J, et al. Role of transcription factor NF-κB in asbestos-induced TNFα response from macrophages. Exp Mol Pathol 1999;66:201–10.

36. Barchowsky A, Roussel RR, Krieser RJ, Mossman BT, Treadwell MD. Expression and activity of urokinase and its receptor in endothelial and pulmonary epithelial cells exposed to asbestos. Toxicol Appl Pharmacol 1998;152:388–96.

37. Driscoll KE, Carter JM, Howard BW, Hassenbein D, Janssen YM, Mossman BT. Crocidolite activates NF-κB and MIP-2 gene expression in rat alveolar epithelial cells. Role of mitochondrial-derived oxidants. Environ Health Perspect 1998;106 Suppl 5:1171–4.

38. Dai J, Churg A. Relationship of fiber surface iron and active oxygen species to expression of procollagen, PDGF-A, TGF-β(1) in tracheal explants exposed to amosite asbestos. Am J Respir Cell Mol Biol 2001;24:427–35.

39. Aldieri E, Orecchia S, Ghigo D, et al. Simian virus 40 infection down-regulates the expression of nitric oxide synthase in human mesothelial cells. Cancer Res 2004;64:4082–4.

40. Yang H, Bocchetta M, Kroczynska B, et al. TNF-α inhibits asbestos-induced cytotoxicity via a NF-κB–dependent pathway, a possible mechanism for asbestos-induced oncogenesis. Proc Natl Acad Sci U S A 2006;103:10397–402.

41. Bocchetta M, Di Resta I, Powers A, et al. Human mesothelial cells are unusually susceptible to simian virus 40-mediated transformation and asbestos cocarcinogenicity. Proc Natl Acad Sci U S A 2000;97:10214–9.

42. Cristaudo A, Foddis R, Vivaldi A, et al. SV40 enhances the risk of malignant mesothelioma among people exposed to asbestos: a molecular epidemiologic case-control study. Cancer Res 2005;65:3049–52.

43. Carbone M, Kratzke RA, Testa JR. The pathogenesis of mesothelioma. Semin Oncol 2002;29:2–17.

44. Carbone M, Emri S, Dogan AU, et al. A mesothelioma epidemic in Cappadocia: scientific developments and unexpected social outcomes. Nat Rev Cancer 2007;7:147–54.

45. Kroczynska B, Cutrone R, Bocchetta M, et al. Crocidolite asbestos and SV40 are cocarcinogens in human mesothelial cells and in causing mesothelioma in hamsters. Proc Natl Acad Sci U S A 2006;103:14128–33.

46. Pass HI, Mew DJ, Carbone M, Donington JS, Baserga R, Steinberg SM. The effect of an antisense expression plasmid to the IGF-1 receptor on hamster mesothelioma proliferation. Dev Biol Stand 1998;94:321–8.

47. Cacciotti P, Strizzi L, Vianale G, et al. The presence of simian-virus 40 sequences in mesothelioma and mesothelial cells is associated with high levels of vascular endothelial growth factor. Am J Respir Cell Mol Biol 2002;26:189–93.

48. Foddis R, De Rienzo A, Broccoli D, et al. SV40 infection induces telomerase activity in human mesothelial cells. Oncogene 2002;21:1434–42.

49. Scheid MP, Woodgett JR. Protein kinases: six degrees of separation? Curr Biol 2000;10:R191–4.

50. Machuca C, Mendoza-Milla C, Cordova E, et al. Dexamethasone protection from TNF-α–induced cell death in MCF-7 cells requires NF-κB and is independent from AKT. BMC Cell Biol 2006;7:9.

51. Madge LA, Pober JS. A phosphatidylinositol 3-kinase/Akt pathway, activated by tumor necrosis factor or interleukin-1, inhibits apoptosis but does not activate NFκB in human endothelial cells. J Biol Chem 2000;275:15458–65.

52. Richmond A, Fan GH, Dhawan P, Yang J. How do chemokine/chemokine receptor activations affect tumorigenesis? Novartis Found Symp 2004;256:74–89; discussion -91, 106–11, 266–9.

53. Mitsiades N, Mitsiades CS, Poulaki V, et al. Molecular sequelae of proteasome inhibition in human multiple myeloma cells. Proc Natl Acad Sci U S A 2002;99:14374–9.

54. Hutchinson J, Jin J, Cardiff RD, Woodgett JR, Muller WJ. Activation of Akt (protein kinase B) in mammary epithelium provides a critical cell survival signal required for tumor progression. Mol Cell Biol 2001;21:2203–12.

55. Spano JP, Bay JO, Blay JY, Rixe O. Proteasome inhibition: a new approach for the treatment of malignancies. Bull Cancer 2005;92:61–6, 945–52.

56. Singh S, Khar A. Activation of NFκB and Ub-proteasome pathway during apoptosis induced by a serum factor is mediated through the upregulation of the 26S proteasome subunits. Apoptosis 2006;11:845–59.

57. Carlotti F, Dower SK, Qwarnstrom EE. Dynamic shuttling of nuclear factor κB between the nucleus and cytoplasm as a consequence of inhibitor dissociation. J Biol Chem 2000;275:41028–34.

58. Sunwoo JB, Chen Z, Dong G, et al. Novel proteasome inhibitor PS-341 inhibits activation of nuclear factor-κB, cell survival, tumor growth, and angiogenesis in squamous cell carcinoma. Clin Cancer Res 2001;7:1419–28.

Correction: Article on Bortezomib Inhibition of Nuclear Factor-KB-Dependent Survival

In the article on Bortezomib's inhibition of nuclear factor-KB-dependent survival and its potent *in vivo* activity in mesothelioma, beginning on page 5942 of the October 1, 2007, issue of *Clinical Cancer Research*, the affiliations for two authors were incorrectly stated. Dr. Andrea Sartore-Bianchi and Dr. Camillo Porta are affiliated with the Institute of Internal Medicine and Medical Oncology, IRCCS Policlinico San Matteo University Hospital, 1-27100 Pavia, Italy. In addition, the current address of Andrea Sartore-Bianchi is as follows: Falck Division of Medical Oncology, Niguarda Ca' Granda Hospital, Milano, Italy.

doi:10.1158/1078-0432.CCR-13-21-COR1

Clinical Cancer Research

Bortezomib Inhibits Nuclear Factor-κB–Dependent Survival and Has Potent *In vivo* Activity in Mesothelioma

Andrea Sartore-Bianchi, Fabio Gasparri, Arturo Galvani, et al.

Clin Cancer Res 2007;13:5942-5951.